Temperature Measurement of a Bridge Rubber Bearing Exposed to Solar Radiation for Long-Term Performance Evaluation

Y. Kitane[1], Paramashanti[2], and Y. Itoh[3]

[1] Assistant Professor, Department of Civil Engineering, Nagoya University, Nagoya, Aichi 464-8603, Japan, E-mail: ykitane@civil.nagoya-u.ac.jp

[2] Graduate Student, Department of Civil Engineering, Nagoya University, Nagoya, Aichi 464-8603, Japan, E-mail: parama@civil.nagoya-u.ac.jp

[3] Professor, Department of Civil Engineering, Nagoya University, Nagoya, Aichi 464-8603, Japan, E-mail: itoh@civil.nagoya-u.ac.jp

ABSTRACT

To understand a daily variation of bearing temperature and examine the effect of solar radiation on the bearing temperature, which is an important piece of information for a long-term performance evaluation of a rubber bearing, field measurements were conducted on a high damping rubber bearing installed in an elevated highway in summer and winter seasons. By using measured solar radiation, a temperature variation in the bearing was examined through the heat transfer analysis. Results from the field measurements show that the difference between the surface temperature and the ambient temperature became significantly large when the surface received direct solar radiation on a sunny day, and that the maximum difference was greater than 20˚C. However, on the bearing surface in the shadow, the surface temperature was close to the ambient temperature, and the maximum difference was only about 2˚C. The heat transfer analysis indicated that the region where temperature was significantly higher than the ambient temperature due to solar radiation was within about 20 mm from the surface, and that in the inner region the rubber temperature did not differ much from the ambient temperature.

Keywords: rubber bearing, temperature, solar radiation, long-term performance, aging

INTRODUCTION

Rubber bearings are now widely used as base isolation bearings in buildings and bridges. It is, however, well known that rubber materials can be damaged and deteriorate by oxygen, ozone, heat, light, oil, and other liquids. As a result of the deterioration process, physical properties of rubbers change over time, which is called *aging*. The aging problems of rubber materials have been studies for some years [1,2,3,4,5,6]. Aging causes rubber to stiffen and its tensile strength and elongation at break to decrease. It has been reported that heat oxidation is one of the major deterioration factors for rubber of bridge rubber bearings [7].

The heat oxidation process is temperature-dependent – the higher the temperature, the faster the material deterioration will be. Since the aging of rubber results in a change of mechanical properties of rubber bearings, including shear stiffness and damping ratio, seismic performance of the bridge system with rubber bearings will also change over time.

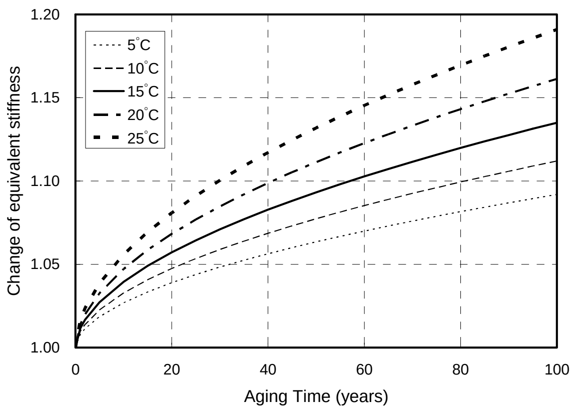

Fig. 1 Change of Equivalent Stiffness of 600 mm Square NR Bearing due to Aging

Itoh et al. [8,9,10] proposed simple methods of analysis to estimate the effect of aging on mechanical properties of natural rubber (NR) and high damping rubber (HDR) bearings based on accelerated aging test results. Since heat oxidation is one of the major deterioration factors for rubbers of bridge bearings, bearing temperature has a significant influence on the deterioration process of rubber. In the proposed methods, bearing temperature is assumed to be equal to the yearly average temperature of the bearing installation site. For example, the change of equivalent stiffness of an NR bearing (600 mm x 600 mm) due to aging can be estimated as shown in Fig. 1 for different average ambient temperatures, where the vertical axis shows a ratio of the equivalent stiffness of an aged bearing to that of a new bearing. Most bridge bearings are usually in the shadow as they are installed between superstructure and substructure. It is, hence, assumed that rubber in bearings has the same temperature as its surrounding ambient temperature. However, as shown in Fig. 2, there are many bearings that are exposed to solar radiation that causes bearing temperature to increase, which may accelerate aging of rubber.

In this study, surface temperatures of a bearing installed in an elevated highway were measured in summer and winter seasons to evaluate the effect of solar radiation on the bearing temperature. In addition, a heat transfer analysis was performed by using simplified boundary conditions based on measured data to examine a temperature variation inside the bearing.

FIELD MEASUREMENT

Bearing of this Study

The bearing is a HDR bearing of 670 mm x 670 mm installed on a concrete pier of an elevated highway system in Nagoya, Japan. Dimensions of the bearing are shown in Fig. 3. The bearing has six rubber layers with a thickness of 26 mm, five layers of inner steel plates with a thickness of 4.5 mm, and two 36 mm thick steel end plates. The bearing has surface NR with a thickness of 10 mm.


Fig. 2 Example of a Bearing Exposed to Sunlight

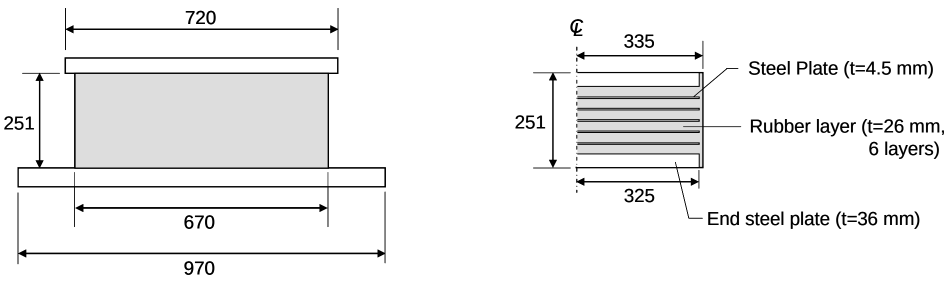

(a) Elevation (b) Vertical section

Fig. 3 Schematic Drawings of the Bearing of this Study (units: mm)

Fig. 4 shows a top view of the concrete pier where the bearing was installed on. The bearing surfaces of the south and west sides can receive sunlight much more than the north and east sides.

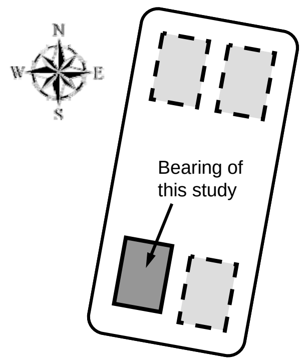

Fig. 4 Top View of Concrete Pier

Measurement Program

The measurement in the summer season was taken from August 25 to September 2, 2007, and from January 18 to January 25, 2008 in winter. Bearing temperatures were measured by using T-type thermocouples with a wire diameter of 0.32 mm, at nine points on the west and east sides, and eight points on the north and south sides. Temperatures of steel girder, bottom and top steel plates, a steel joint protection, and the top surface of concrete pier were also measured on each side of the bearing. Steel joint protections are steel blocks to control bearing displacement in the transverse direction of the bridge, and they are located in front of the south and north surfaces of the bearing. Measurement locations are shown in Fig. 5. In addition, solar radiations were measured on the south and north sides using pyranometers with sensitivity of 7 mV/kW/m^2 for wave lengths of 305-2,800 nm. Ambient temperature was also measured by thermocouple.

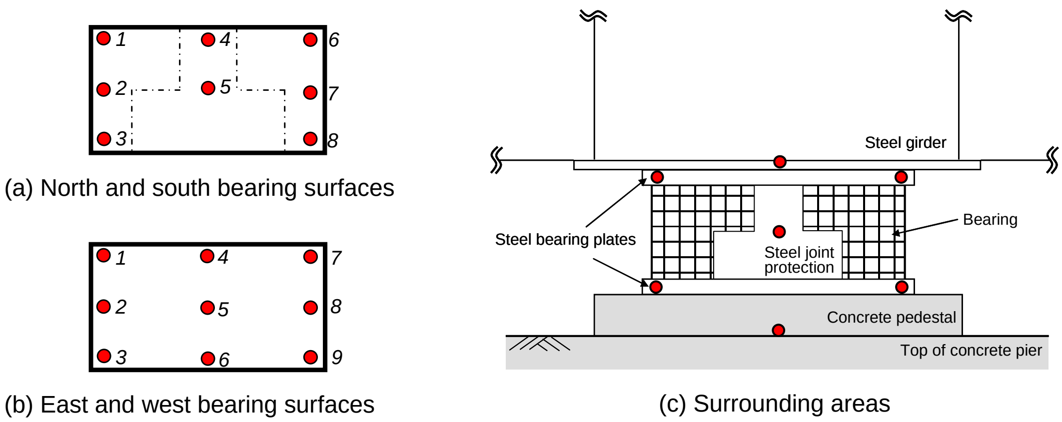

(a) North and south bearing surfaces

(b) East and west bearing surfaces

(c) Surrounding areas

Fig. 5 Temperature Measurement Locations

Results and Discussions

Table 1 summarizes measured temperatures. Fig. 6 shows time histories of temperatures and solar radiation from the summer measurement. During the summer measurement, the maximum, minimum, and average ambient temperature were 35˚C, 23˚C, and 28˚C, respectively, while in winter, they were 10˚C, 0˚C, and 5˚C, respectively. There were four sunny days, three cloudy days, and two rainy days in the summer measurement, and four sunny days, three cloudy days, and one rainy day in the winter measurement.

By comparing Fig. 6 (a), (b), and (d), it is apparent that bearing surface temperatures were affected by solar radiation. With the bearing orientation shown in Fig. 4, the east surface receives solar radiation in the early morning, the south side does during the day, and the east side does in the afternoon. When a bearing surface receives solar radiation on a sunny day, the difference between the surface temperature and the ambient temperature becomes significantly large. In the summer measurement, the maximum bearing temperature was 55˚C, which was 20˚C higher than the ambient temperature at the same time. A greater difference was found in winter, as the maximum bearing surface temperature was 46˚C, which was 36˚C higher than the ambient temperature. The maximum bearing temperature occurred on the west side in summer and on the south side in winter.

However, differences between average ambient temperatures and average bearing surface temperatures over the measurement period in summer were only 2.0˚C on the east side, 2.5˚C on the west side, 2.6˚C on the south side, and 1.3˚C on the north side. In winter, the differences between the average values were slightly greater, but of the same order. When average temperatures of one sunny day are concerned, differences between average ambient and bearing surface temperatures in summer were 2.5˚C, 3.6˚C, 3.6˚C, and 1.3˚C on the east, west, south, and north sides, respectively, and in winter the maximum difference was 6.5˚C on the south side. It should also be noted that the surface temperature of the north side that was in the shadow was very close to the ambient temperature even when other surfaces had very high temperatures due to solar radiation, implying that solar radiation on one surface does not affect temperature of other surfaces significantly.

Temperatures of the surrounding areas were measured to understand boundary conditions of the bearing. Results show similar variations to those of bearing surface

Table 1 Summary of Temperature Measurement (˚C)

		Summer				Winter			
		Max.	Min.	Ave.	Ave. of Aug. 27	Max.	Min.	Ave.	Ave. of Jan. 19
Ambient		34.8	23.3	28.2	31.4	10.3	0.4	5.0	5.3
Bearing	North	36.7	24.7	29.5	32.7	12.2	2.1	6.0	7.3
	South	43.6	24.0	30.8	35.0	35.1	1.4	8.7	11.7
	East	38.8	24.9	30.2	33.9	22.6	1.8	7.1	9.4
	West	54.6	24.3	30.7	35.0	31.7	1.5	6.9	8.1
Steel Girder	North	36.9	23.8	28.7	31.8	13.4	0.7	5.3	6.2
	South	45.4	25.2	31.7	35.8	18.3	2.5	7.3	9.3
	East	39.1	23.8	29.5	33.3	14.7	0.5	6.3	8.1
	West	44.1	23.7	29.8	33.5	18.9	0.3	6.1	7.5
Concrete Pier	North	35.2	23.7	28.7	31.2	9.2	2.8	5.6	6.2
	South	44.8	23.4	30.1	34.3	21.2	0.0	6.7	8.7
	East	45.8	23.1	29.9	33.3	15.5	2.6	6.4	7.6
	West	45.6	24.2	30.6	34.6	16.7	0.8	5.9	6.9

temperatures, that is, temperatures differ significantly from the ambient temperature only when they are exposed to solar radiation. The difference between average temperature of each measured location and average ambient temperature ranged from 1˚C to 3˚C for the east, south, and west sides in summer, while the difference ranged from 1˚C to 2˚C for those sides in winter. On the north side, temperatures of surrounding areas were similar to the ambient temperature.

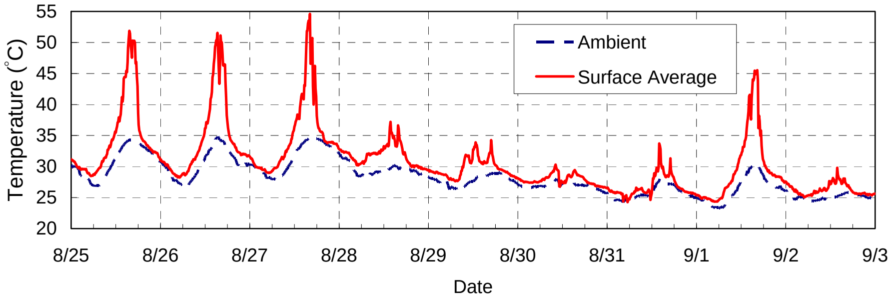

(a) West bearing surface

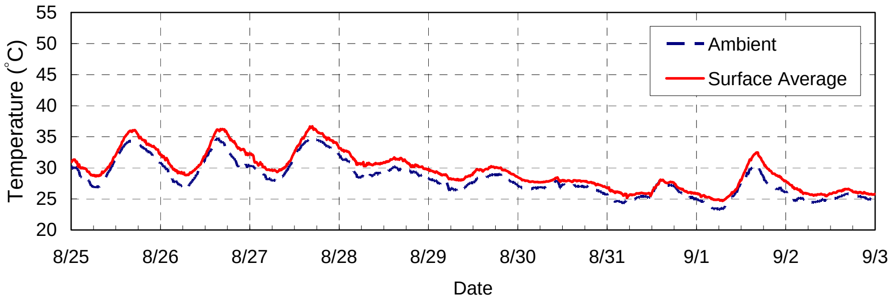

(b) North bearing surface

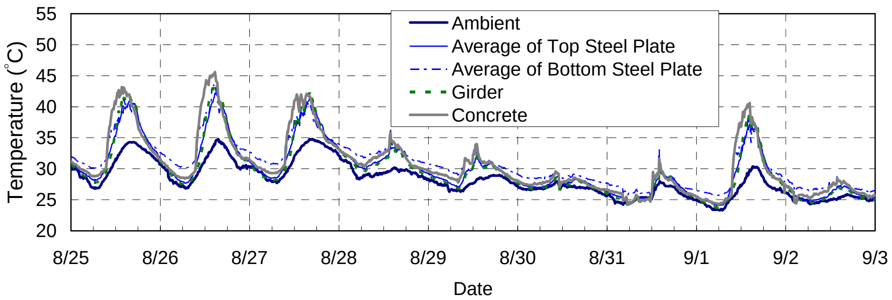

(c) Surrounding areas (west side)

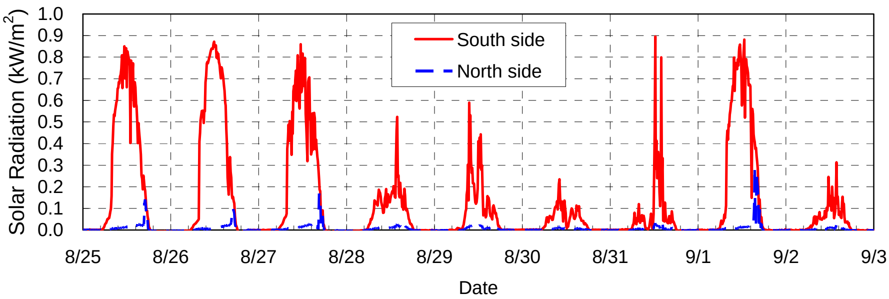

(d) Solar radiation

Fig. 6 Field Measurement Results (summer)

HEAT TRANSFER ANALYSIS

Analytical Model

To understand a temperature variation in a bearing exposed to solar radiation, a heat transfer analysis of the bearing was performed using finite element techniques. A half of the bearing shown in Fig. 3 was modeled in a general-purpose finite element program ABAQUS [11], as shown in Fig. 7. Material properties used in the analysis are shown in Table 2.

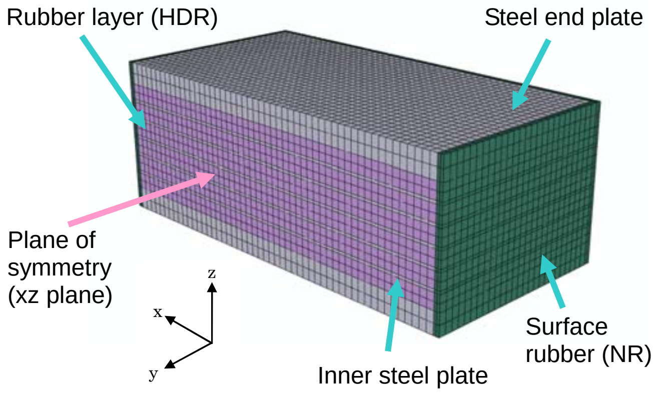

Fig. 7 Finite Element Model of the Rubber Bearing

Table 2 Material Properties Used in Heat Transfer Analysis

	Thermal conductivity [W/(m・K)]	Specific heat [J/(kg・K)]	Density [kg/m^3]
NR	0.27	1,688	1,100
HDR	0.34	1,619	1,160
Steel	62.3	455	7,850

Boundary Conditions

Surface numbers in the model and the type of boundary conditions considered on each surface are shown in Fig. 8. It is assumed that Surface 2 receives heat energy from solar radiation and its temperature increases. In the analysis, a temperature time history shown in Fig. 9 was applied to Surface 2, which is a piecewise linear approximation of the measured temperature variation on the south surface in the summer measurement. On Surface 1, a temperature time history based on the measured north surface temperatures was applied. Temperatures on Surfaces 1 and 2 were applied until temperatures of the bearing reached a steady state condition. On Surface 3, convection between the rubber surface and air was considered. A film coefficient used was 11.61 W/(m^2・K) [12]. A symmetry boundary condition was used on Surface 4. Although for Surfaces 5 and 6, there should be heat transfer through these surfaces in the actual bearing, an insulated boundary condition was assumed in the analysis, resulting in a less heat loss from the bearing than the actual conditions

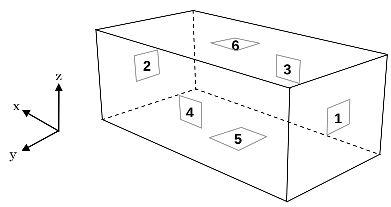

Surface	B.C.
1	Temperature
2	Temperature
3	Convection
4	Insulated
5	Insulated
6	Insulated

Fig. 8 Surface Numbers and Types of Boundary Conditions

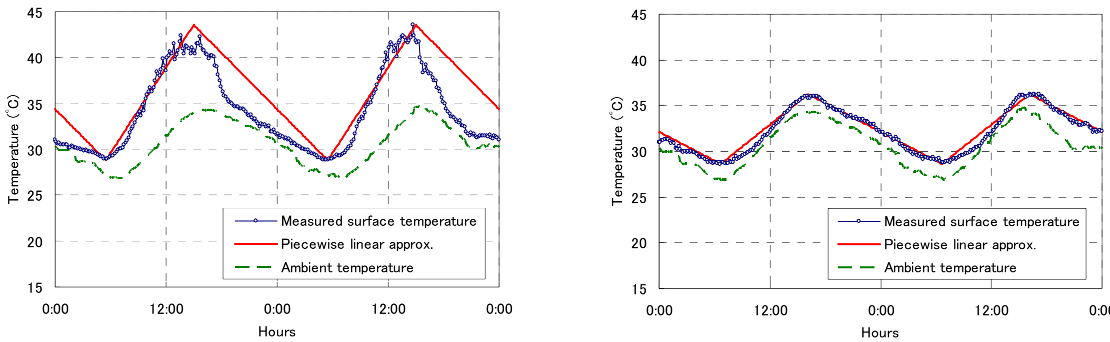

(a) Surface 2 (south surface) (b) Surface 1 (north surface)

Fig. 9 Applied Temperature Time History

Results and Discussions

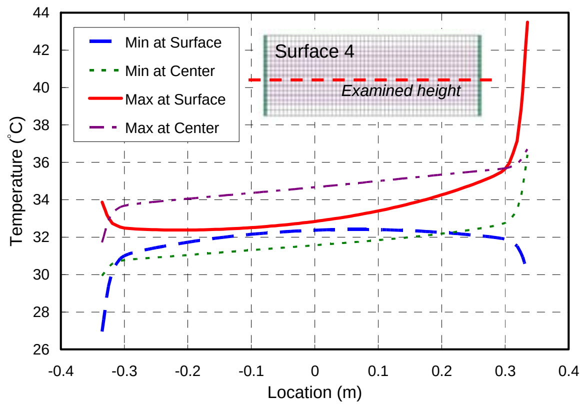

Fig. 10 Temperature Variation at Mid-height on Surface 4

Fig. 10 shows temperature variations in the bearing at the mid-height on Surface 4, which is a plane of symmetry, at four time instances: 1) minimum temperature on the surface, 2) minimum temperature at the center, 3) maximum temperature on the surface, and 4) maximum temperature at the center. The horizontal axis of Fig. 10 shows a distance from the center of the bearing. It is obvious from Fig. 10 that a temperature variation inside the bearing is significantly smaller than that on the surface. The difference between the maximum and minimum temperatures at the center was only 3.1˚C. The average temperature at the center was higher than the average ambient temperature by only 2.6˚C. The region where temperature can be significantly affected by solar radiation was found to be about 20 to 30 mm from the surface.

CONCLUSIONS

It is concluded from the field measurements that bearing surface temperature is significantly higher than ambient temperature when the surface is exposed to solar radiation. However, when the bearing surface does not receive solar radiation because it is in the shadow or because it is cloudy or rainy, the difference between the surface and ambient temperatures becomes small. When daily average temperatures are compared, the difference between bearing surface and ambient temperatures is not more than several degrees Celsius, even on the surfaces that receive solar radiation during the day.

The heat transfer analysis showed that the region where temperature was significantly affected by solar radiation was only within 20 to 30 mm from the surface exposed to solar radiation, and that temperature at the center increased from the ambient temperature by only a few degrees Celsius. However, boundary conditions used in the analysis were simplified from the actual ones, and it is necessary in the future to verify the analytical model and boundary conditions by measuring temperature variations in the bearing exposed to solar radiation.

REFERENCES

1) Braden, M. and Gent, A.N. (1960), "The attack of ozone on stretched rubber vulcanizates. I. The rate of cut growth," *Journal of Applied Polymer Science*, Vol. 3, pp. 90-100.
2) Blackman, E.J. and McCall, E.B. (1969), "Relationship between the structures of natural rubber vulcanizates and their thermal and oxidative aging," *Rubber Chemistry and Technology*, Buffalo, New York, October 14-17, pp. 651-661.
3) Koike, M., Tanaka, K. and Hioki, S. (1979), "Weatherability of elastomeric roofing membranes," *Journal of Asian Architecture & Building Engineering*, A.I.J., No. 285, pp.15-22 (in Japanese).
4) Zlata, H. M. and Jasenka, J. (2000), "Change of network structure of natural rubber vulcanizate with thermal aging," *Macromolecular Materials and Engineering*, No. 283, pp. 21-25.
5) Sugimoto, H., Mizoe, M., Yamamoto, Y. and Ikenaga M. (2001), "Research on low temperature resistance of the natural rubber bearing," *Journal of Structural and Earthquake Engineering*, JSCE, No.693/VI-53, pp. 73-86 (in Japanese).
6) Wei, Y. T., Nasdala, L., Rothert, H. and Xie, Z. (2004), "Experimental investigations on the dynamic mechanical properties of aged rubbers," *Polymer Testing*, pp. 447-453.
7) Itoh, Y., Gu, H.S., Satoh, K. and Kutsuna, Y. (2006), "Experimental investigation on aging behaviors of rubbers used for bridge bearings," *Journal of Structural and Earthquake Engineering*, JSCE, Vol. 62, No. 1, pp. 176-190.
8) Itoh, Y., Satoh, K., Gu, H.S., and Yamamoto, Y. (2006), "Study on the deterioration characteristics of natural rubber bearings," *Journal of Structural and Earthquake Engineering*, JSCE, Vol. 62, No. 2, pp. 255-266 (in Japanese).
9) Itoh, Y., Gu, H.S., Satoh, K. and Yamamoto, Y. (2006), "Long-term deterioration of high damping rubber bridge bearing," *Journal of Structural and Earthquake Engineering*, JSCE, Vol. 62, No. 3, pp. 595-607.
10) Paramashanti, Itoh, Y., Kitane, Y., and Gu, H. (2007), "Long-term performance evaluation of high damping rubber bearings by accelerated thermal oxidation test," *Proc. 2nd International Conference on Advances in Experimental Structural Engineering*, Shanghai, China, December 4-6, Paper No. 07120113, pp. 664-671.
11) ABAQUS Inc. (2007): *ABAQUS ver. 6.7 Documentation, ABAQUS Analysis User's Manual*.
12) Uruta, H., Yamazaki, T., Ohsima, T., and Nakamura, M. (2004), "Experiments and numerical analysis on response of internal temperature of high damping rubber bridge bearing under low temperature," *Journal of Structural and Earthquake Engineering*, JSCE, No. 773/I-69, pp. 113-123.